

A Step in Between: $[\text{Sn}_3\text{Bi}_3]^{5-}$ and Its Structural Relationship to $[\text{Sn}_3\text{Bi}_5]^{3-}$ and $[\text{Sn}_4\text{Bi}_4]^{4-}$

Ute Friedrich and Nikolaus Korber^{*[a]}

Extraction of "RbSnBi" in liquid ammonia yielded the cluster anion $[\text{Sn}_3\text{Bi}_5]^{3-}$, which could be crystallized in the compound $[\text{Rb}@[2.2.2]\text{crypt}]_3[\text{Sn}_3\text{Bi}_5] \cdot 8.87 \text{NH}_3$. This anion is found to be derived from the formerly reported $[\text{Sn}_4\text{Bi}_4]^{4-}$ by the formal substitution of one tin atom by bismuth. In contrast, the extraction of "RbSn₂/Rb₃Bi₂" in liquid ammonia yielded the anion $[\text{Sn}_3\text{Bi}_3]^{5-}$ in the compound $\text{Rb}_6[\text{Sn}_3\text{Bi}_3][\text{Sn}_4]_{1/4} \cdot 6.75 \text{NH}_3$. The structural correlation of the two novel clusters indicates that $[\text{Sn}_3\text{Bi}_3]^{5-}$ might be an intermediate of the reaction pathway to $[\text{Sn}_3\text{Bi}_5]^{3-}$ and $[\text{Sn}_4\text{Bi}_4]^{4-}$. Each cluster is investigated by means of the electron localization function and further characterization was performed by using ESI-MS.

The field of homoatomic polyanions of heavier main-group elements, the so-called Zintl anions, has been investigated since the beginning of modern chemistry. The insight into what kind of molecular structures may be built if only one element is employed forms part of our fundamental knowledge of main-group chemistry. Representative cluster anions that are present in a large number of the compounds known to date, and which can serve as building blocks for bigger clusters, are $[\text{T}_4]^{4-}$ and $[\text{T}_9]^{x-}$ ($x=3, 4$) for group 14 elements ($T=\text{Si-Pb}$) or $[\text{Pn}_7]^{3-}$ and $[\text{Pn}_{11}]^{3-}$ for group 15 elements ($\text{Pn}=\text{P-Bi}$).^[1] From these basic structures, heteroatomic clusters originate through partial substitution. The type of element chosen for the substitution is a cardinal point in influencing properties such as the size and the solubility of the anions. Until now, among others, the anions $[\text{Sn}_2\text{Pn}_2]^{2-}$, $[\text{Pb}_2\text{Pn}_2]^{2-}$ ($\text{Pn}=\text{Sb, Bi}$), $[\text{Si}_{4-x}\text{Ge}_x]^{4-}$ ($x=1, 2$), $[\text{EBi}_3]^{2-}$ ($E=\text{In, Ga}$), $[\text{Sn}_3\text{Sb}_4]^{6-}$, $[\text{T}_7\text{Bi}_2]^{2-}$ ($T=\text{Sn, Pb}$), $[\text{Sb}_2\text{Ge}_7]^{2-}$, and $[\text{In}_4\text{Bi}_5]^{3-}$ were obtained by the formal exchange of one or more atoms of the homoatomic cage.^[2-4] They could be characterized through X-ray diffraction and were primarily synthesized by using mixed precursor phases. In reactions of solutions of homoatomic polyanions with metal

organic compounds or metal halogenides anions like $[\text{TlT}_9]^{3-}$ ($T=\text{Ge, Sn}$), $[\text{InPn}_{14}]^{3-}$, $[\text{PbPn}_{15}]^{3-}$, and $[\text{TlPn}_7]^{2-}$ ($\text{Pn}=\text{P, As}$) were obtained, in which the homoatomic $[\text{Pn}_7]$ and $[\text{T}_9]$ structural motives are conserved.^[5]

Focusing on the tinbismuthides, this field is found to be scarcely investigated, as only three anions have been characterized to date, namely $[\text{Sn}_2\text{Bi}_2]^{2-}$, $[\text{Sn}_7\text{Bi}_2]^{2-}$, and $[\text{Sn}_4\text{Bi}_4]^{4-}$.^[3,4,6] The $[\text{Sn}_2\text{Bi}_2]^{2-}$ anion was initially synthesized by Corbett et al. in the compound $[\text{K}@[2.2.2]\text{crypt}]_2[\text{Sn}_2\text{Bi}_2]\text{-en}$ in 1982, as one of the first heteroatomic Zintl anions.^[3b] This compound was reproduced by Dehnen et al. and used as a starting material for reactions with transition metal and lanthanide metal complexes.^[7] In this manner, ternary anions like $[\text{Ni}_2\text{Sn}_7\text{Bi}_5]^{3-}$, $[\text{Ln}@[\text{Sn}_7\text{Bi}_7]^{4-}$, $[\text{Ln}@[\text{Sn}_4\text{Bi}_9]^{4-}$ ($\text{Ln}=\text{La, Ce}$), and $[\text{Pd}_3\text{Sn}_8\text{Bi}_6]^{4-}$ were obtained. In the course of the reaction between $[\text{K}@[2.2.2]\text{crypt}]_2[\text{Sn}_2\text{Bi}_2]\text{-en}$ and ZnPh_2 , the binary anion $[\text{Sn}_7\text{Bi}_2]^{2-}$ crystallized together with $[\text{Zn}_6\text{Sn}_3\text{Bi}_8]^{4-}$.^[4] In 2012, we were able to add $[\text{Sn}_4\text{Bi}_4]^{4-}$ in the compound $[\text{Cs}@[18]\text{crown-6}]_4[\text{Sn}_4\text{Bi}_4] \cdot 12 \text{NH}_3$ as part of the very short list of known anions with the shape of a monocapped nortricyclane-like cage. Herein, we report the first synthesis of the similarly built anion $[\text{Sn}_3\text{Bi}_5]^{3-}$ in $[\text{Rb}@[2.2.2]\text{crypt}]_3[\text{Sn}_3\text{Bi}_5] \cdot 8.87 \text{NH}_3$ (**1**) and propose a possible correlation of both clusters with the, likewise, new $[\text{Sn}_3\text{Bi}_3]^{5-}$ anion, which we could crystallize from liquid ammonia in the compound $\text{Rb}_6[\text{Sn}_3\text{Bi}_3][\text{Sn}_4]_{1/4} \cdot 6.75 \text{NH}_3$ (**2**).

Cluster compound **1** is obtained by the extraction of a solid-state starting material of the nominal composition "RbSnBi" with liquid ammonia in the presence of $[2.2.2]\text{crypt}$ (4,7,13,16,21,24-hexa-oxa1,10-diazabicyclo[8.8.8]hexacosane). After approximately six weeks of storage at 236 K, black, block-shaped crystals form. A single-crystal X-ray structure determination revealed that compound **1** contains the novel anionic cluster $[\text{Sn}_3\text{Bi}_5]^{3-}$, which is disordered over two positions in the crystal structure, as shown in Figure 1 (top). Its structure compares to the previously reported $[\text{Sn}_4\text{Bi}_4]^{4-}$ anion if the apical position is exchanged by a bismuth atom. Thus, the $[\text{Sn}_3\text{Bi}_5]^{3-}$ anion consists of a formal nortricyclane-like $[\text{Sn}_2\text{Bi}_5]^{5-}$ cage with the two tin atoms in the basal plane and one additional Sn^{2+} cation capping the Sn1–Sn3–Bi4–Bi3 plane to form a tin triangle (Figure 1 bottom). The average atomic distances (d) in $[\text{Sn}_3\text{Bi}_5]^{3-}$ are $d(\text{Sn}-\text{Sn})=3.1202(16) \text{ \AA}$, $d(\text{Sn}-\text{Bi})=2.9688(14) \text{ \AA}$, and $d(\text{Bi}-\text{Bi})=2.9724(7) \text{ \AA}$. The height (h) of the cluster from the apical bismuth atom to the center of the basal plane is $4.1848(6) \text{ \AA}$, whereas the shortest distance of the capping atom Sn2 to the Sn1–Sn3–Bi4–Bi3 plane is $1.8568(7) \text{ \AA}$. The individual distances from Sn2 to Sn1/Sn3 and Bi3/Bi4 are $3.096 \text{ \AA}/3.120 \text{ \AA}$ and $2.998 \text{ \AA}/3.018 \text{ \AA}$. All values match those found in the structurally related $[\text{Sn}_4\text{Bi}_4]^{4-}$ anion, in which only the apical bismuth atom Bi5 is substituted by a tin atom.

[a] U. Friedrich, Prof. Dr. N. Korber
Fakultät für Chemie und Pharmazie
Universität Regensburg
Universitätsstraße 31
93053 Regensburg (Germany)
E-mail: nikolaus.korber@ur.de

Supporting Information for this article can be found under <http://dx.doi.org/10.1002/open.201600037>.

© 2016 The Authors. Published by Wiley-VCH Verlag GmbH & Co. KGaA. This is an open access article under the terms of the Creative Commons Attribution-NonCommercial-NoDerivs License, which permits use and distribution in any medium, provided the original work is properly cited, the use is non-commercial and no modifications or adaptations are made.

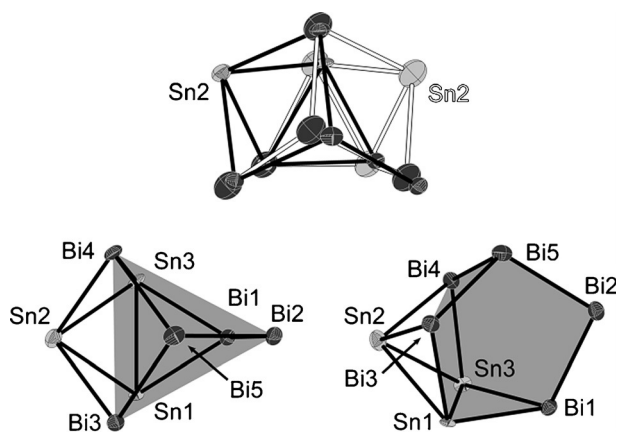


Figure 1. Top) Disorder of the $[\text{Sn}_3\text{Bi}_3]^{3-}$ anion in the crystal structure with a 120° rotation; disorder is depicted as full and open bonds. Bottom-left) Top view of the anion. Bottom-right) Side view of the anion; tin atoms: light grey, bismuth atoms: dark grey.

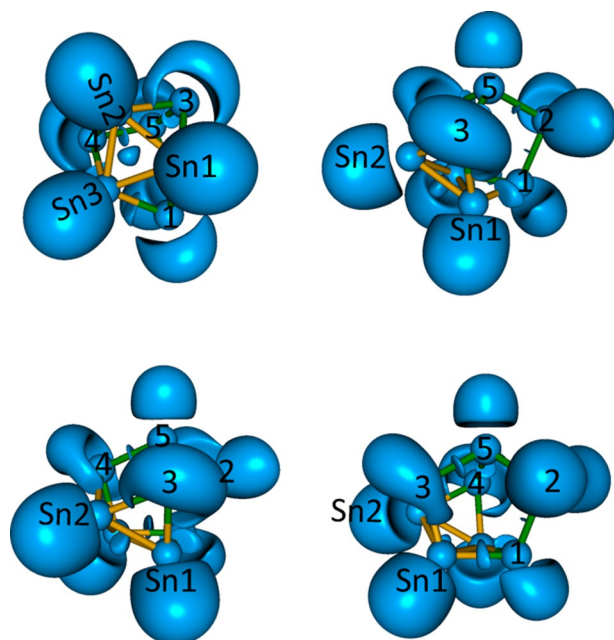


Figure 2. ELF of $[\text{Sn}_3\text{Bi}_3]^{3-}$ depicted at the isosurface value $\eta = 0.63$, showing mono-, di-, and trisynaptic basins; bismuth atoms: green, labeled with atom numbers; tin atoms: yellow.

The electron localization function (ELF) for different orientations of the $[\text{Sn}_3\text{Bi}_3]^{3-}$ anion is shown in Figure 2 for isosurface value $\eta = 0.63$. Besides the core and monosynaptic basins, di- and trisynaptic basins can be found. The monosynaptic basins representing lone pairs are populated with $2.18\text{--}2.28e^-$ at the tin atoms and $2.28\text{--}2.55e^-$ at Bi2 and Bi5. A significantly higher population is found for Bi1, Bi3, and Bi4 with $2.75\text{--}2.99e^-$. The higher population for monosynaptic bismuth basins is attributed to the higher electronegativity in contrast to the tin atoms. The difference among the bismuth atoms originates from the number of less electronegative tin atoms neighboring the particular bismuth atoms. Disynaptic basins,

which represent two-center bonds, are found for all Sn–Bi and Bi–Bi bonds. The attractors of these basins are generally found a little way from the bonding axis of the atoms, indicating some cluster tension. The integral over the electron density of the disynaptic basins provides populations between 1.47 and $1.68e^-$. The attractor of the trisynaptic basin is located inside the Sn1–Sn2–Sn3 triangle and is populated with $1.57e^-$. The presence of the three-center bond explains the elongated homoatomic tin distances of about $3.1202(16)$ Å found by single-crystal X-ray diffraction.

For the preparation of compound **2**, an equimolar mixture of the solid-state phases “ RbSn_2 ” and “ Rb_3Bi_2 ” is extracted with liquid ammonia in the presence of [2.2.2]crypt. Within 8 weeks at 236 K, **2** crystallizes in the form of black hexagonal rods from the reddish brown reaction mixture. Single-crystal X-ray diffraction provided evidence for the formation of another unprecedented anion, $[\text{Sn}_3\text{Bi}_3]^{5-}$. This anion consists of a tin triangle with one bismuth atom bridging every edge (Figure 3). The

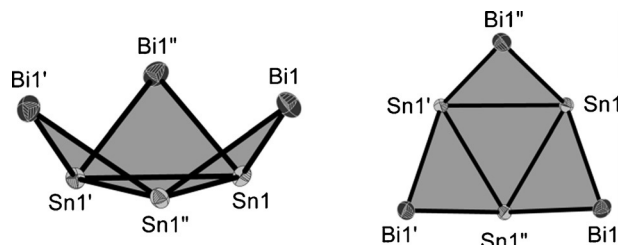


Figure 3. Left) Side view of the $[\text{Sn}_3\text{Bi}_3]^{5-}$ anion. Right) Top view; tin atoms: light grey, bismuth atoms: dark grey.

anion shows C_3 symmetry in the crystal structure; neglecting distortions caused by packing effects, it can be described in C_{3v} symmetry. The Sn–Sn atomic distance is $3.1244(16)$ Å and Sn–Bi bonds are $2.9807(12)$ Å and $2.9975(11)$ Å. The shortest distance between two bismuth atoms is $4.897(12)$ Å [$r_{\text{vdW}}(\text{Bi}) = 1.535$ Å]. The opening angle, α , between the tin triangle and each of the other triangles is $138.95(3)^\circ$. In the crystal structure, the anion is surrounded by rubidium cations, forming a framework with channel-like cavities. These channels are filled with $[\text{Sn}_4]^{4-}$ tetrahedra, rubidium cations, and ammonia molecules, all showing disorder.

Three of the five negative charges of the anion can formally be assigned to the two bonded bismuth atoms. The remaining two charges are to be shared equally between the three tin atoms. Furthermore, the $[\text{Sn}_3\text{Bi}_3]^{5-}$ anion can be described by Wade–Mingos rules. It has $(3 \times 4 + 3 \times 5 + 5) = 32$ valence electrons and $(32 - 6 \times 2) / 2 = 10$ skeletal electron pairs. Taking into account the six vertices, the anion is a *hypho* cluster ($n + 4$). The formal derivation of the $[\text{Sn}_3\text{Bi}_3]^{5-}$ anion from the corresponding nine-atom *closo*-type cluster is shown in Figure 4.

The electronic situation is illustrated by the ELF, which is shown in Figure 5 for different orientations of the anion at $\eta = 0.63$. Each bismuth atom has two monosynaptic basins with populations of $2.44\text{--}2.52e^-$. Each tin atom has one monosynaptic basin populated with $2.17\text{--}2.23e^-$. The higher population of the monosynaptic bismuth basins is again rationalized

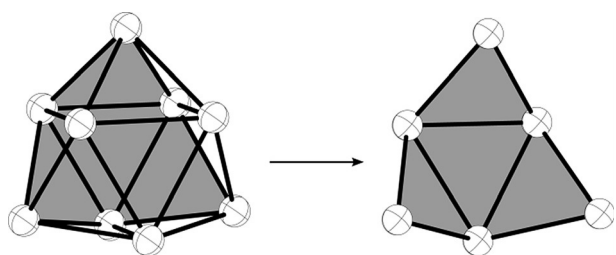


Figure 4. Derivation of the $[\text{Sn}_3\text{Bi}_3]^{5-}$ anion from the corresponding *closo*-type cluster. Left) Tricapped trigonal prism with the position of the six-membered fragment highlighted in grey. Right) Six-membered fragment after formal removal of the three front vertices of the trigonal prism.

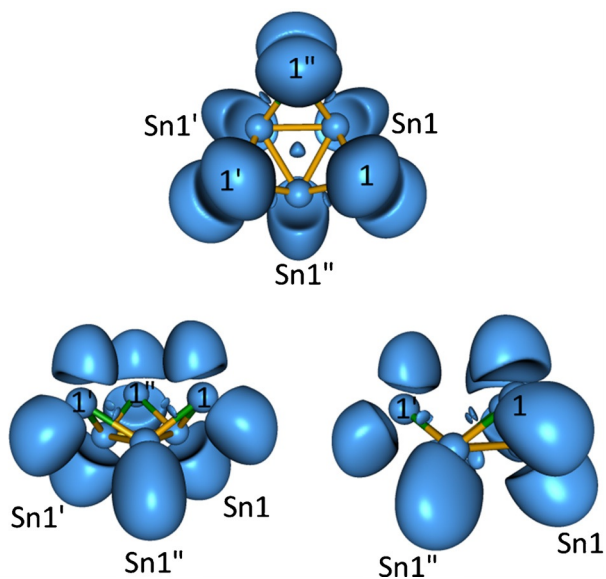


Figure 5. ELF of $[\text{Sn}_3\text{Bi}_3]^{5-}$ at the isosurface value $\eta = 0.63$, showing mono-, di-, and trisynaptic basins; bismuth atoms: green, labeled with atom numbers; tin atoms: yellow. Top) Top view of the anion. Bottom) Different side views.

by the higher electronegativity of the bismuth atoms. An attractor for a disynaptic basin can be found close to every Sn–Bi bond. The integral over the electron density has the average value of $1.40e^-$, the trisynaptic basin inside the tin triangle is populated with $1.46e^-$. Table 1 gives an overview of the basin populations, comparing anions $[\text{Sn}_3\text{Bi}_3]^{5-}$, $[\text{Sn}_3\text{Bi}_3]^{3-}$, and $[\text{Sn}_4\text{Bi}_4]^{4-}$. The overall population in all three anions is shifted from bonding basins to valence basins; a shift that is already known for such heavy polyanions and is slightly more pro-

| Table 1. Population of bonding basins in the $[\text{Sn}_3\text{Bi}_3]^{5-}$, $[\text{Sn}_3\text{Bi}_3]^{3-}$, and $[\text{Sn}_4\text{Bi}_4]^{4-}$ anions. | | | |
|--|---------------------------------|---------------------------------|---------------------------------|
| Basin | $[\text{Sn}_3\text{Bi}_3]^{5-}$ | $[\text{Sn}_3\text{Bi}_3]^{3-}$ | $[\text{Sn}_4\text{Bi}_4]^{4-}$ |
| V(Sn–Sn–Sn) | 1.46 | 1.57 | 1.53 |
| V(Sn–Bi) | 1.39–1.41 | 1.52–1.68 | 1.45–1.73 |
| V(Bi–Bi) | – | 1.47–1.60 | 1.42 |
| V(Sn) | 2.17–2.23 | 2.18–2.28 | 2.17–2.27 |
| V(Bi) | 2.44–2.52 | 2.28–2.99 | 2.31–3.05 |

nounced for $[\text{Sn}_3\text{Bi}_3]^{5-}$. This might indicate that, through reorganization processes in solution, the system tends to form anions with a more electron precise situation. The populations of monosynaptic tin basin $V(\text{Sn})$ stay almost constant for the different sized clusters, whereas the populations at the bismuth atoms $V(\text{Bi})$ adapt to the varying bonding situations in the anions, as these are directly involved in the formation of new bonds.

As no covalent bonds are present between the bismuth atoms, it can be assumed that the stabilization of the $[\text{Sn}_3\text{Bi}_3]^{5-}$ ion in the observed geometry arises from the repulsion of the free electron pairs, and that the $[\text{Sn}_3\text{Bi}_3]^{5-}$ anion might be an intermediate of the reaction pathway to bigger clusters. The formation of $[\text{Sn}_4\text{Bi}_4]^{4-}$ and $[\text{Sn}_3\text{Bi}_3]^{3-}$ support this assumption, as these anions contain the $[\text{Sn}_3\text{Bi}_3]$ fragment (Figure 6). Fur-

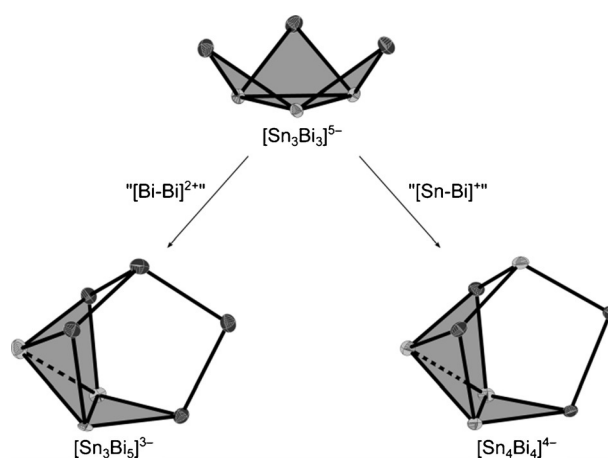


Figure 6. The $[\text{Sn}_3\text{Bi}_3]^{5-}$ anion as possible intermediate of the reaction pathway to the anions $[\text{Sn}_3\text{Bi}_3]^{3-}$ and $[\text{Sn}_4\text{Bi}_4]^{4-}$; tin atoms: light grey, bismuth atoms: dark grey.

thermore, the main characteristics of the geometry and the electronic structure of the $[\text{Sn}_3\text{Bi}_3]^{5-}$ cluster are present in both anions. Starting from the $[\text{Sn}_3\text{Bi}_3]^{5-}$ cluster, the addition of either a “Sn–Bi” or a “Bi–Bi” dumbbell completes the corresponding eight-atom clusters. Upon the formal introduction of the dumbbell, the angle between the basal plane and the tin triangle is opened slightly from $138.95(3)^\circ$ in $[\text{Sn}_3\text{Bi}_3]^{5-}$ to $139.764(11)^\circ$ in $[\text{Sn}_4\text{Bi}_4]^{4-}$ and $141.81(4)^\circ$ in $[\text{Sn}_3\text{Bi}_3]^{3-}$. The angles between the tin triangle and the two remaining triangle planes are reduced by about 10° in both anions. Thus, the distances between atoms Bi3 and Bi4 are reduced to about 4.4 \AA , as compared to $4.897(12) \text{ \AA}$ in $[\text{Sn}_3\text{Bi}_3]^{5-}$. The distances of Bi3/Bi4 to Bi1 are about 4.6 \AA for both eight-atom clusters. A similar transformation from $[\text{K}@\{2.2.2\}\text{crypt}\}_2[\text{Sn}_2\text{Bi}_2]\text{-en}$ to $[\text{K}@\{2.2.2\}\text{crypt}\}_2[\text{Sn}_7\text{Bi}_7]\text{-en-tol}$ was reported by Lips and Dehnen in 2009.^[4]

For ESI-MS characterization, both syntheses were performed in ethylenediamine/dimethylformamide. For “RbSnBi”, among others, the singly charged fragments $[\text{Sn}_3\text{Bi}_3]^-$, $[\text{Sn}_4\text{Bi}_4]^-$, and $[\text{Sn}_3\text{Bi}_5]^-$ could be detected, whereas the reaction mixture of “RbSn₂/Rb₃Bi₂” decomposes so rapidly that only the $[\text{Sn}_2\text{Bi}_2]^-$

fragment could be identified in solution. The signal of $[\text{Sn}_3\text{Bi}_3]^-$ at $m/z = 1400.8$ is overlaid by another fragment that might be $[\text{Sn}_{10}\text{Bi}]^-$ with $m/z = 1396.0$. Additional characterization was performed for solutions of LiSnBi , showing, among others, the $[\text{Sn}_3\text{Bi}_3]^-$, $[\text{Sn}_3\text{Bi}_3]^-$, and $[\text{LiSn}_4\text{Bi}_4]^-$ fragments. Owing to the higher stability of the reaction mixture, the quality of the signals increased, but the aforementioned problem remained.

In summary, we were able to crystallize and structurally characterize the novel $[\text{Sn}_3\text{Bi}_3]^{5-}$ anion, which has a crown-like structure. The anion is probably an intermediate of the reaction pathway to clusters like $[\text{Sn}_3\text{Bi}_5]^{3-}$ and $[\text{Sn}_4\text{Bi}_4]^{4-}$. The main characteristics of the geometry and the electronic structure of the $[\text{Sn}_3\text{Bi}_3]^{5-}$ anion are maintained in the latter two anions. The $[\text{Sn}_3\text{Bi}_3]^{3-}$ anion was structurally characterized for the first time and can formally be derived from the $[\text{Sn}_4\text{Bi}_4]^{4-}$ anion by exchange of the apical tin atom by bismuth.

Experimental Section

$\text{Rb}@[2.2.2]\text{crypt}]_3[\text{Sn}_3\text{Bi}_3] \cdot 8.87 \text{NH}_3$ (**1**): "RbSnBi" (165 mg, 0.2 mmol) and $[2.2.2]\text{crypt}$ (113 mg, 0.3 mmol) were weighed into a baked-out Schlenk tube. Afterwards, dry ammonia (about 10 mL) was condensed, forming a red-brown solution. The Schlenk tube was stored at 236 K. **1** was obtained in about 10% crystalline yield.

$\text{Rb}_6[\text{Sn}_3\text{Bi}_3][\text{Sn}_4]_{1/4} \cdot 6.75 \text{NH}_3$ (**2**): "RbSn₂" (323 mg, 1 mmol), "Rb₃Bi₂" (674 mg, 1 mmol), and $[2.2.2]\text{crypt}$ (80 mg, 0.2 mmol) were weighed in a baked-out Schlenk tube and ammonia (about 10 mL) was condensed. The red-brown reaction solution was stored at 236 K. **2** was obtained in 10–20% crystalline yield.

Single-crystal X-ray diffraction data for both compounds were recorded on a SuperNova (Agilent technologies) at 123 K with Mo radiation ($\lambda_{\text{av}} = 0.71073 \text{ \AA}$).^[8] The crystals were selected under perfluoroalkylether and mounted on a loop (MiTeGen, 200 μm) in a stream of cool nitrogen.

The structures were solved with olex.solve and refined on F^2 by using SHELXL.^[9] For illustrations, the program Diamond was used.^[10]

Crystal data for **1**: $M_r = 2937.95 \text{ g mol}^{-1}$, space group $P-1$, $\mu = 12.020 \text{ mm}^{-1}$, $\rho_{\text{calc}} = 2.131 \text{ g cm}^{-3}$, $a = 12.8297(1) \text{ \AA}$, $b = 16.4868(2) \text{ \AA}$, $c = 24.4432(3) \text{ \AA}$, $\alpha = 92.99(1)^\circ$, $\beta = 104.564(1)^\circ$, $\gamma = 111.947(1)^\circ$, $V = 4579.41(9) \text{ \AA}^3$, $Z = 2$, 71 547 measured reflections, 18 665 independent reflections; $R_{\text{int}} = 0.034$, $R_1 = 0.031$, and $wR_2 = 0.077$ for $I > 2\sigma(I)$; $R_1 = 0.038$ and $wR_2 = 0.081$ for all data; $S = 1.018$, $\Delta\rho_{\text{max}} = 3.25 \text{ e \AA}^{-3}$, $\Delta\rho_{\text{min}} = -2.43 \text{ e \AA}^{-3}$. The disorder of the $[\text{Sn}_3\text{Bi}_3]^{3-}$ anion was modeled with a 0.87:0.13 ratio.

Crystal data for **2**: $M_r = 1709.09 \text{ g mol}^{-1}$, space group $P-3c1$, $\mu = 28.011 \text{ mm}^{-1}$, $\rho_{\text{calc}} = 3.478 \text{ g cm}^{-3}$, $a = b = 15.5790(4) \text{ \AA}$, $c = 15.5289(6) \text{ \AA}$, $\alpha = \beta = 90^\circ$, $\gamma = 120^\circ$, $V = 3264.0(2) \text{ \AA}^3$, $Z = 4$, 10 309 measured reflections, 1927 independent reflections; $R_{\text{int}} = 0.062$, $R_1 = 0.040$, and $wR_2 = 0.105$ for $I > 2\sigma(I)$; $R_1 = 0.062$ and $wR_2 = 0.108$ for all data; $S = 0.942$, $\Delta\rho_{\text{max}} = 6.74 \text{ e \AA}^{-3}$, $\Delta\rho_{\text{min}} = -1.66 \text{ e \AA}^{-3}$. For the handling of the disorder, see the Supporting Information.^[11]

Computational studies were performed by using the program package TURBOMOLE.^[12] Geometry optimization was done without symmetry restrictions. All atoms were described with def2-TZVPP basis sets and effective core potentials were used for a better description of relativistic effects (Sn: ecp-28-mdf, Bi: ecp-60-mdf). The

COSMO model was applied with $\epsilon = 16.9$; all other default options of the program were accepted. For the calculations of the ELF, the program DGRID was used, and for its representations, the program gOpenMol was used.^[13]

ESI-MS characterization experiments were performed on a TSQ 7000 spectrometer from Thermoquest Finnigan in the negative-ion mode. All anions were detected as singly charged species.

Acknowledgements

We thank the Fonds der chemischen Industrie (FCI) for financial support.

Keywords: ammonia · cage molecules · polyanions · tinbismuthide · Zintl anions

- [1] a) S. Scharfe, F. Kraus, S. Stegmaier, A. Schier, T. F. Fässler, *Angew. Chem. Int. Ed.* **2011**, *50*, 3630; *Angew. Chem.* **2011**, *123*, 3712; b) S. P. R. Turber-vill, J. M. Goicoechea, *Chem. Rev.* **2014**, *114*, 10807–10828; c) N. Korber, A. Fleischmann, *J. Chem. Soc. Dalton Trans.* **2001**, 383–385; d) K. Wiesler, K. Brandl, A. Fleischmann, N. Korber, *Z. Anorg. Allg. Chem.* **2009**, *635*, 508–512; e) A. Ugrinov, S. C. Sevov, *Appl. Organomet. Chem.* **2003**, *17*, 373–376; f) L. Xu, S. C. Sevov, *J. Am. Chem. Soc.* **1999**, *121*, 9245–9246; g) J. D. Corbett, P. A. Edwards, *J. Am. Chem. Soc.* **1977**, *99*, 3313–3317; h) T. F. Fässler, R. Hoffmann, *J. Chem. Soc. Dalton Trans.* **1999**, 3339–3340; i) L. G. Perla, A. G. Oliver, S. C. Sevov, *Inorg. Chem.* **2015**, *54*, 872–875; j) A. C. Reber, A. Ugrinov, A. Sen, M. Qian, S. N. Khanna, *Chem. Phys. Lett.* **2009**, *473*, 305–311; k) B. Weinert, A. R. Eulenstein, R. Ababei, S. Dehnen, *Angew. Chem. Int. Ed.* **2014**, *53*, 4704–4708; *Angew. Chem.* **2014**, *126*, 4792–4797; l) V. Miluykov, A. Kataev, O. Sinyashin, P. Lönnecke, E. Hey-Hawkins, *Z. Anorg. Allg. Chem.* **2006**, *632*, 1728–1732; m) R. C. Haushalter, B. W. Eichhorn, A. L. Rheingold, S. J. Geib, *J. Chem. Soc. Chem. Commun.* **1988**, 1027–1028; n) J. Curda, W. Carrillo-Cabrera, A. Schmeding, K. Peters, M. Somer, H. G. von Schnering, *Z. Anorg. Allg. Chem.* **1997**, *623*, 929–936.
- [2] a) R. Ababei, J. Heine, M. Holyńska, G. Thiele, B. Weinert, X. Xie, F. Weigend, S. Dehnen, *Chem. Commun.* **2012**, *48*, 11295–11297; b) F. Lips, I. Schellenberg, R. Pöttgen, S. Dehnen, *Chem. Eur. J.* **2009**, *15*, 12968; c) S. C. Critchlow, J. D. Corbett, *Inorg. Chem.* **1985**, *24*, 979–981; d) L. Xu, S. C. Sevov, *Inorg. Chem.* **2000**, *39*, 5383; e) M. Waibel, O. Pecher, B. Mausolf, F. Haarmann, T. F. Fässler, *Eur. J. Inorg. Chem.* **2013**, 5541–5546; f) M. M. Gillett-Kunnath, A. G. Oliver, S. C. Sevov, *J. Am. Chem. Soc.* **2011**, *133*, 6560.
- [3] a) F. Lips, M. Raupach, W. Massa, S. Dehnen, *Z. Anorg. Allg. Chem.* **2011**, *637*, 859; b) S. C. Critchlow, J. D. Corbett, *Inorg. Chem.* **1982**, *21*, 3286–3290.
- [4] F. Lips, S. Dehnen, *Angew. Chem.* **2009**, *121*, 6557–6560.
- [5] a) R. C. Burns, J. D. Corbett, *J. Am. Chem. Soc.* **1982**, *104*, 2804–2810; b) D. Rios, M. M. Gillett-Kunnath, J. D. Taylor, A. G. Oliver, S. C. Sevov, *Inorg. Chem.* **2011**, *50*, 2373–2377; c) C. M. Knapp, J. S. Large, N. H. Rees, J. M. Goicoechea, *Dalton Trans.* **2011**, *40*, 735–745.
- [6] U. Friedrich, M. Neumeier, C. Koch, N. Korber, *Chem. Commun.* **2012**, *48*, 10544–10546.
- [7] a) F. Lips, S. Dehnen, *Angew. Chem.* **2011**, *123*, 986–990; b) F. Lips, R. Clérac, S. Dehnen, *J. Am. Chem. Soc.* **2011**, *133*, 14168–14171; c) F. Lips, M. Holyńska, R. Clérac, U. Linne, I. Schellenberg, R. Pöttgen, F. Weigend, S. Dehnen, *J. Am. Chem. Soc.* **2012**, *134*, 1181–1191.
- [8] CrysAlisPro Software Version 1.171.37.35, Agilent Technologies UK Ltd., Oxford (UK), **2011**.
- [9] a) G. Sheldrick, *Acta Cryst. A* **2008**, *64*, 112–122; b) O. V. Dolomanov, L. J. Bourhis, R. J. Gildea, J. A. K. Howard, H. Puschmann, *J. Appl. Crystallogr.* **2009**, *42*, 339–341.
- [10] K. Brandenburg, Vol. DIAMOND, Version 3.2k, Crystal Impact GbR, Bonn (Germany), **2014**.

- [11] CCDC 1440853 and 1440854 contain the supplementary crystallographic data for this paper. These data can be obtained free of charge from The Cambridge Crystallographic Data Centre.
- [12] TURBOMOLE V6.3 2011, A Development of University of Karlsruhe and Forschungszentrum Karlsruhe GmbH, 1989–2007, TURBOMOLE GmbH, since 2007, 2010.
- [13] M. Kohout, DGrid, version 4.6, Radebeul, 2011; E. H. K. Boyd, L. Laakso-
nen, gOpenMol, version 3.00, 1997–2005.

Received: April 25, 2016
Published online on May 25, 2016